1. Temperature and density fluctuations in the inner Orion Nebula

1.1. Deriving diagnostic line ratios from WFC3 filter images

Note: this is similar to what I wrote in the the calibration draft, but specifically tailored to line ratios rather than equivalent widths.

The WFC3 camera is equipped with filters that effectively target important nebular diagnostic lines. Each filter, with label j, is characterized by an effective transmission profile, or throughput, T_λ^j, which gives the wavelength-dependent conversion factor between the number of photons arriving at the *HST* entrance aperture (nominal radius: 120 cm) and the number of electrons registered by the CCD, accounting for occultation by the secondary mirror, all other optical and quantum efficiencies, and the amplifier gain. The peak value of the filter transmission profile is denoted T_m^j, with typical values of 0.2–0.3, and the "rectangular width" of the profile is defined as

$$W_j = (T_\mathrm{m}^j)^{-1} \int_0^\infty T_\lambda^j \, d\lambda \qquad [W_j] = \text{Å}. \tag{1}$$

Extensive and continuing on-orbit calibration of the filters has been carried out (*citation of relevant ISRs*) using white dwarf standard stars. However, since these are flat featureless continuum sources, the calibration is only sensitive to the product $W_j T_\mathrm{m}^j$. Emission lines from photoionized regions are intrinsically much narrower than even the narrowest WFC3 filters, so the transmission of such a line, with label i, is independent of T_λ^j and depends only on the throughput at the line wavelength: $T_i^j \equiv T_\lambda^j(\lambda = \lambda_i)$.

The calibration of these filters is discussed in detail in a companion paper (**?**), where it is

For the strongest lines, such as [N II]6583 In order to accurately calculate emission line ratios from WFC3 images, it is important to properly account for the contamination

1.2. Deriving T_e, n_e from line ratios

1.3. Analysis of fluctuations in T_e, n_e

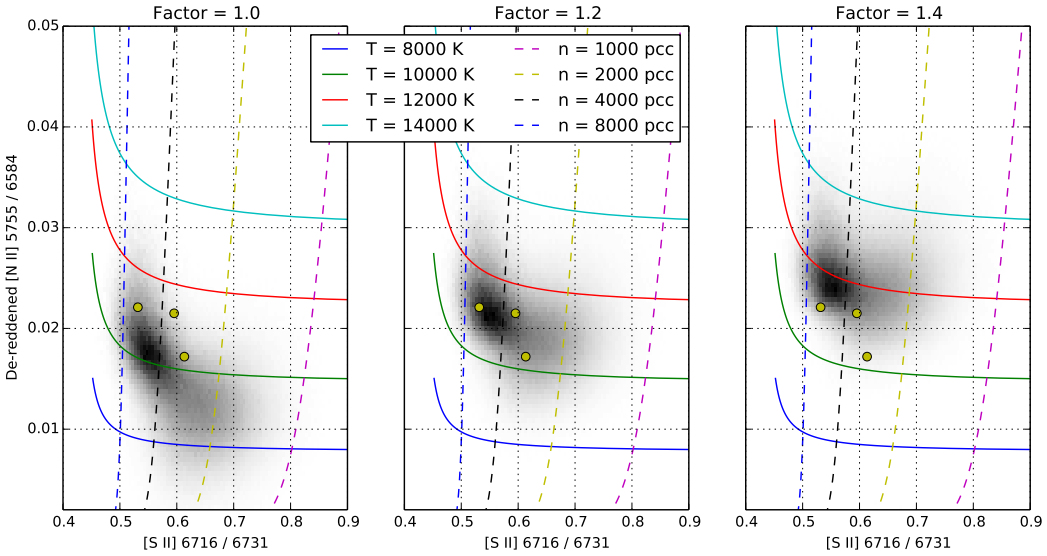

Fig. 1.— Distribution of line ratios

(*a*)

(*b*)

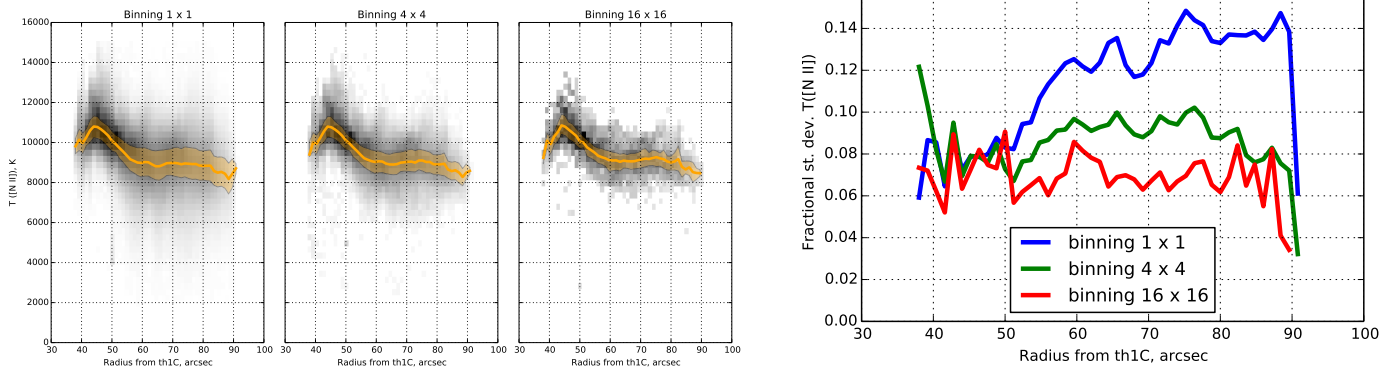

Fig. 2.— (*a*) Temperature distribution as a function of radius for different binnings. (*b*) Standard deviation of temperatures as a function of radius for different binnings.

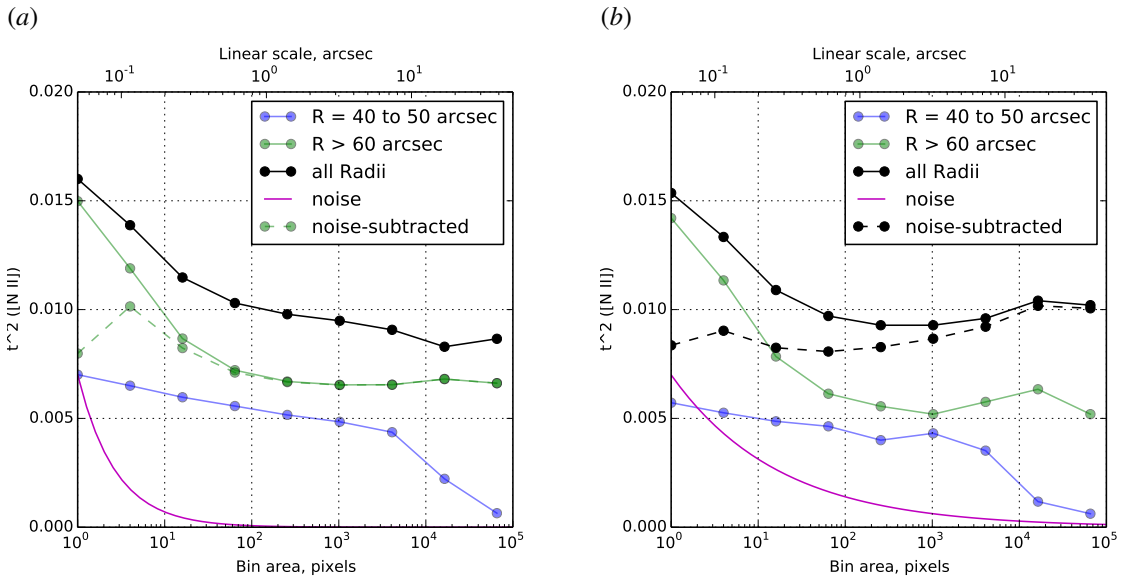

Fig. 3.— Scale-dependence of temperature fluctuations: t^2 as a function of binning. (*a*) Variance of $T_e/\bar{T}_e$ for the entire image (black line) and two subsamples: an annulus centered on the high-temperature region (blue line) and the more distant, fainter regions (green line). The magenta line is an estimate of the noise contribution to the full sample, and the dashed black line is the result of subtracting the noise from the observed values. (*b*) Same as *a* but using a "robust" estimator of the variance, based on the interquartile range.

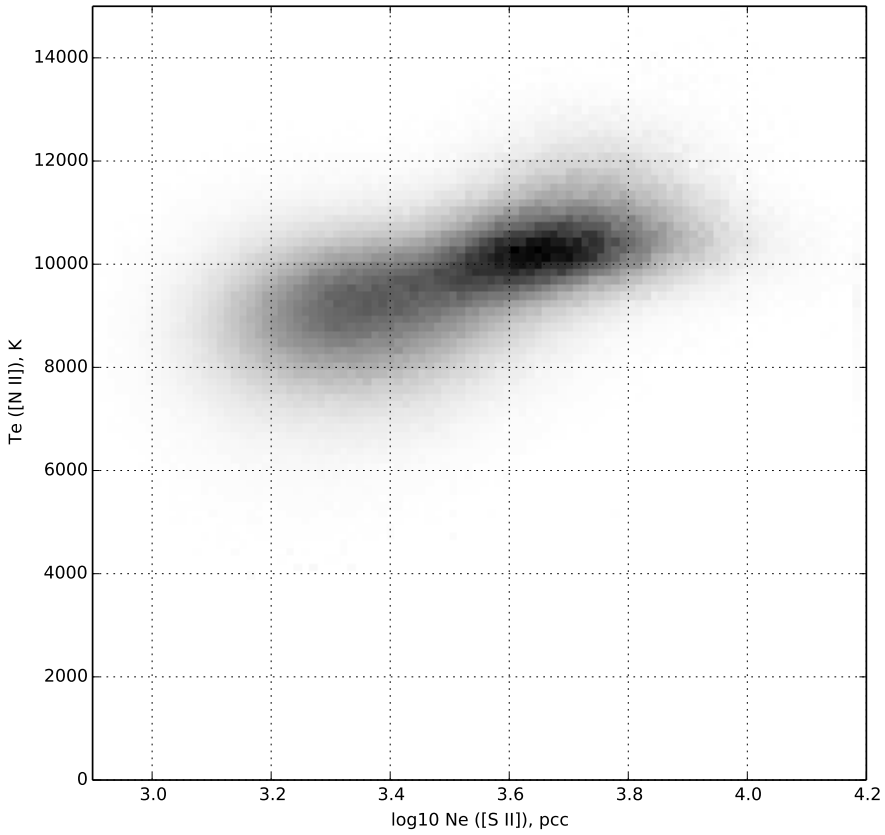

Fig. 4.— Joint distribution of temperature and electron density for low ionization regions.

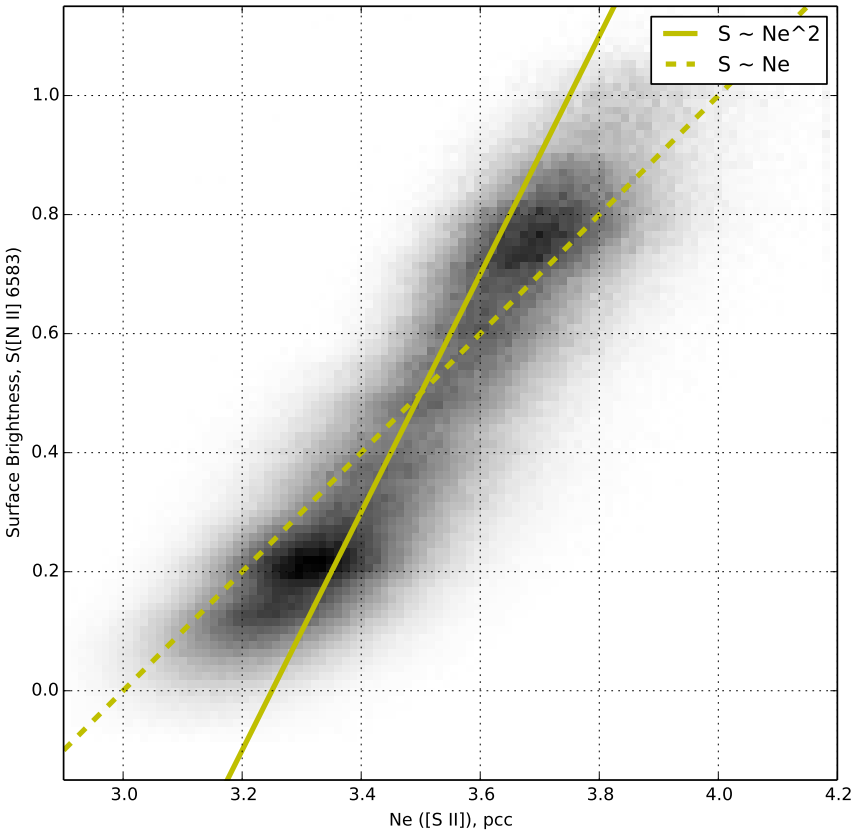

Fig. 5.— Correlation between [S II] density and [N II] surface brightness.